DNA AND CELL BIOLOGY
Volume 42, Number 11, 2023

Pp. 697–708
DOI: 10.1089/dna.2023.0169

Homozygous Mutations in *GDAP1* and *MFN2* Genes Resulted in Autosomal Recessive Forms of Charcot–Marie–Tooth Disease in Consanguineous Pakistani Families

Muhammad Asif,[1,2,*] Chien-Chun Chiou,[3,*] Malik Fiaz Hussain,[2,*] Manzoor Hussain,[4] Zureesha Sajid,[1,5] Muhammad Gulsher,[6] Afifa Raheem,[2] Adil Khan,[7] Nasreen Nasreen,[8] Andrzej Kloczkowski,[9,10] Mubashir Hassan,[9] Furhan Iqbal,[2] and Chien-Chin Chen[11–14]

Charcot–Marie–Tooth disease (CMT) is a heritable neurodegenerative disease of peripheral nervous system diseases in which more than 100 genes and their mutations are associated. Two consanguineous families Dera Ghazi Khan (PAK-CMT1-DG KHAN) and Layyah (PAK-CMT2-LAYYAH) with multiple CMT-affected subjects were enrolled from Punjab province in Pakistan. Basic epidemiological data were collected for the subjects. Nerve conduction study (NCS) and electromyography (EMG) were performed for the patients. Whole-exome sequencing (WES) followed by Sanger sequencing was applied to report the genetic basic of CMT. The NCS findings revealed that sensory and motor nerve conduction velocities for both families were <38 m/s. EMG presented denervation, neuropathic motor unit potential, and reduced interference pattern of peripheral nerves. WES identified that a novel nonsense mutation (c. 226 G>T) in *GADP1* gene and a previously known missense mutation in *MFN2* gene (c. 334 G>A) cause CMT4A (Charcot–Marie–Tooth disease type 4A) in the PAK-CMT1-DG KHAN family and CMT2A (Charcot–Marie–Tooth disease type 2A) in the PAK-CMT2-LAYYAH family, respectively. Mutations followed Mendelian pattern with autosomal recessive mode of inheritance. Multiple sequence alignment by Clustal Omega indicated that mutation-containing domain in both genes is highly conserved, and *in situ* analysis revealed that both mutations are likely to be pathogenic. We reported that a novel nonsense mutation and a previously known missense mutation in *GAPD1* gene and *MFN2* gene, respectively, cause CMT in consanguineous Pakistani families.

Keywords: Charcot–Marie–Tooth disease, WES, Sanger sequencing, consanguineous families, Pakistan

[1]Institute of Molecular Biology and Biotechnology. Bahauddin Zakariya University, Multan, Pakistan.
[2]Institute of Zoology, Bahauddin Zakariya University, Multan, Pakistan.
[3]Department of Dermatology, Ditmanson Medical Foundation Chia-Yi Christian Hospital, Chiayi, Taiwan.
[4]Orthopedic Unit 1, Nishter Medical University Multan, Pakistan.
[5]Department of Biotechnology, Institute of Biochemistry, Biotechnology and Bioinformatics, Baghdad-ul-Jadeed Campus, The Islamia University of Bahawalpur, Bahawalpur, Pakistan.
[6]Children Hospital and Institute of Child Health, Multan, Pakistan.
[7]Department of Botany and Zoology, Bacha Khan University, Charsadda, Pakistan.
[8]Department of Zoology, Abdul Wali Khan University, Mardan, Pakistan.
[9]The Steve and Cindy Rasmussen Institute for Genomic Medicine, Nationwide Children's Hospital, Columbus, Ohio, USA.
[10]Department of Pediatrics, The Ohio State University, Columbus, Ohio, USA.
[11]Department of Pathology, Ditmanson Medical Foundation Chia-Yi Christian Hospital, Chiayi, Taiwan.
[12]Department of Cosmetic Science, Chia Nan University of Pharmacy and Science, Tainan, Taiwan.
[13]Ph.D. Program in Translational Medicine, Rong Hsing Research Center for Translational Medicine, National Chung Hsing University, Taichung, Taiwan.
[14]Department of Biotechnology and Bioindustry Sciences, College of Bioscience and Biotechnology, National Cheng Kung University, Tainan, Taiwan.
*These authors share the first authorship.

Introduction

Charcot–Marie–Tooth disease (CMT) is a group of heterogeneous genetic diseases that cause damage to the peripheral nerves that transmit brain signals to the body and bring information from the body back to the brain (Higuchi and Takashima, 2023). CMT can develop during every part of life, but progressive muscular weakness usually becomes noticeable during early child or adulthood; as the longer nerves are affected first, the symptoms usually begin in the feet and lower legs, and in the later stages, fingers, hands, and arms of patients are affected (Kanwal et al., 2021). The severity of symptoms can vary greatly among individuals and even among family members with the disease and gene mutation (Zambon et al., 2017). Several types of CMT have been documented, and these types share some of the disease symptoms, but they vary from each other due to different patterns of inheritance, age of onset, and whether the axon or myelin sheath is involved or not (Zambon et al., 2017).

A number of molecular and cellular mechanisms have been reported causing CMT, and these mechanisms have reported problems associated with myelin assembly, cytoskeletal structure, myelin-specific transcription factor, proteasome and protein aggregation, axonal transport, tRNA synthetases and RNA metabolism, and ion channel (Higuchi and Takashima, 2023). A number of studies have been documented to report the genetic basis of CMT, and these studies have either used next-generation sequencing or targeted the specific genes by PCR, which were previously known to be associated with CMT, followed by DNA sequencing (Pisciotta et al., 2021). Inbreeding is a common social attribute in Pakistan, and it is causing an unusually high number of genetic mutations in local population resulting in a number of physical and mental disabilities in children of consanguineous marriages (Mustafa et al., 2020).

A few studies have already reported the peripheral neuropathies in Pakistani patients, and most of the subjects enrolled in these studies were harboring recessive homozygous mutations due to consanguineous marriages of their parents (Houlden et al., 2008; Kanwal et al., 2021; Pedurupillay et al., 2016; Wright et al., 2020; Zambon et al., 2017). In these studies, various CMT types were reported, including distal hereditary motor neuropathy or the spinal CMT (Houlden et al., 2008), CMT2 or spinal muscular atrophy with respiratory distress type 1 (SMARD1) (Pedurupillay et al., 2016), CMT4B1 (demyelination; Zambon et al., 2017), CMT4J and Yunis–Varón syndrome (Wright et al., 2020), and CMT2A2B (axonal dysfunction; Kanwal et al., 2021).

We applied the whole-exome sequencing (WES) followed by Sanger sequencing approach to report the genetic basis of CMT in a couple of Pakistani consanguineous families that were enrolled from two different regions in Punjab province. We reported that a novel nonsense mutation in *GDAP1* gene and a previously known missense mutation in *MFN2* gene cause CMT in enrolled families.

Materials and Methods

Ethical approval

Experimental protocols were reviewed and approved by the ethical committee at Bahauddin Zakariya University, Multan (Pakistan) (approval number: IPAB/Bio Ethics/21-12).

Recruitment of family and collection of blood samples

We enrolled two consanguineous Pakistani families one each from Dera Ghazi Khan (PAK-CMT1-DG KHAN) and Layyah (PAK-CMT2-LAYYAH) districts in Punjab province where multiple members suffer from CMT. Before data and blood sample collection, we obtained the written informed consent from all the participants. The written informed consent was provided by the parents for the minors involved in the study.

Epidemiological and clinical data were collected by interviewing each subject and/or their parents (Supplementary Data S1 CMTI patient data). Onset age was determined by interviewing the parents about when the symptoms, such as distal muscle weakness or foot deformity, first appeared. Blood samples were collected from five unaffected and five affected individuals from family PAK-CMT1-DG KHAN (Fig. 1A). While blood samples were collected from four CMT patients and five unaffected siblings from family PAK-CMT2-LAYYAH (Fig. 1B).

Electrophysiological assessments

Motor and sensory impairments were measured in two patients from family PAK-CMT1-DG KHAN (V-4 and V-5) and in two patients from family PAK-CMT2-LAYYAH (IV-4 and IV-6). Motor conduction velocities of the median, ulnar, bilateral musculocutaneous, peroneal, and tibial nerves were determined by surface stimulation followed by recording using electrodes. Motor nerve conduction velocities (MNCVs) of the median and ulnar nerves were determined by stimulation at the elbow and wrist. In the same way, the MNCVs of peroneal and tibial nerves were determined by stimulation at the ankle. F-waves were also recorded for motor nerves. Sensory nerve conduction velocities (SNCVs) were obtained from a finger–wrist segment for median and ulnar nerves, and were also recorded for sural nerve. Electromyography (EMG) was carried out for the first dorsal interosseous (FDI), abductor pollicis brevis (ABP), transverse abdominis (TA), vastus lateralis (VL), brachioradialis, and biceps muscles with concentric needle electrodes by using Neuropack S1 (MEB-9400).

Whole-exome sequencing

Genomic DNA was extracted using commercial kit (Qiagen, Germany) following the instructions that were provided by the manufacturer along with the kit. One control and one patient were selected for WES from both the PAK-CMT1-DG KHAN (V-1 and V-5) and PAK-CMT2-LAYYAH (III-2 and IV-4) families (Fig. 1A, B). WES and resultant data were analyzed as reported elsewhere (Zhou et al., 2014). ANNOtate VARiation was used for variant annotation. Candidate variants that fulfilled the following criteria were selected: (1) variant should be nonsynonymous or they should be in splice sites within six base pairs of an exon; (2) variant should have minor allele frequency <1% in Kaviar, gnomAD, and in-house databases; and (3) variant should co-segregated with the phenotype of enrolled family.

Sanger sequencing

The candidate variant was validated on DNA of all available family members by Sanger sequencing. PCR

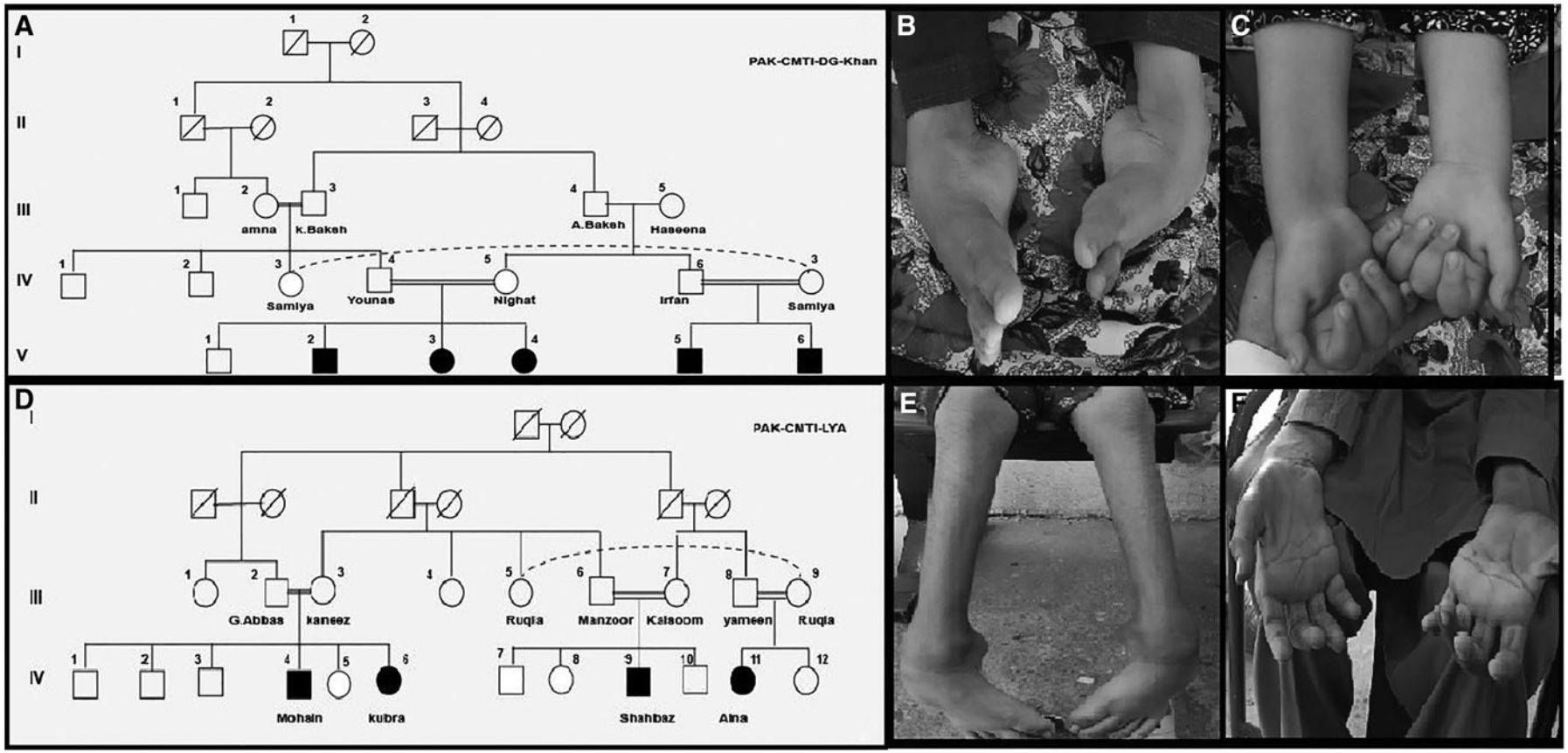

FIG. 1. Pedigree and clinical manifestations. Pedigrees of a consanguineous Pakistani families segregating autosomal recessive form of Charcot–Marie–Tooth disease **(A, D)**. Affected individuals presenting pes cavus and bowed legs **(B, E)** and affected hands with bowed arms **(C, F)**.

products were sequenced using Big Dye Terminator v.3.1 (ABI Thermo Fisher) on ABI 3730.

In silico *mutation prediction*

In silico analyses to predict the mutation effect were performed using the following programs: ENCoM (http://bcb.med.usherbrooke.ca/encom) (Frappier et al., 2015), DUET (http://structure.bioc.cam.ac.uk/duet) (Pires et al., 2014a), mCSM (http://structure.bioc.cam.ac.uk/mcsm) (Pires et al., 2014b), and SDM (http://www-cryst.bioc.cam.ac.uk/~sdm/sdm.php) (Worth et al., 2011).

Multiple sequence alignment

The ganglioside-induced differentiation-associated protein 1 (GDAP1) and Mitofusin-2 (MNF2) protein sequences from various species were downloaded from Ensemble (https://asia.ensembl.org/index.html). Clustal Omega was used for the analysis of these downloaded multiple sequences. Gonnet PAM 250 matrix was used to report the protein sequence homology.

Computational protein modeling

The three-dimensional (3D) structures of both GDAP1 and truncated proteins were predicted through Swiss model approach separately (https://swissmodel.expasy.org). The complete protein structure of GDAP1 and truncated proteins with 358 and 75 amino acids (AA) was utilized to run the predicted models. The template GDAP1 had 100% sequence similarity, 23–302 range, and query coverage value of 0.78. Similarly, for truncated protein, GDAP1 protein was selected with different PDBID 7b2g.1.A having 100% sequence similarity, 23–75 range, and 1.0 query coverage. Models were built based on the target–template alignment using ProMod3 (Studer et al., 2021).

Coordinates that are conserved between the target and the template were copied from the template to the model. Insertions and deletions were remodeled using a fragment library. Side chains were then rebuilt. Finally, the geometry of the resulting model was regularized using a force field. Moreover, the structural evaluations of both predicted models were confirmed through VADAR server (http://vadar.wishartlab.com). Furthermore, the Ramachandran plot analysis was tested through MolProbity server (http://molprobity.biochem.duke.edu) to check their outliers and favored residues configurations. Finally, superimposition of both predicted structures was carried out by UCSF Chimera 1.10 tool (Pettersen et al., 2004).

MNF2 protein structure prediction

The mutated crystal structure of MNF2 was not available in the protein data bank (PDB) (http://www.rcsb.org). Therefore, a homology modeling-based approach was employed to predict the MNF2 (V112M) mutated structure using template PDBIDs 6JFM. Furthermore, the selected mutated structure was used to predict its effects on the protein structure and associated disorders through DynaMut, an online server that predicts the impact of mutations on protein conformation, flexibility, and stability (Rodrigues et al., 2018).

Results

Phenotype of the subjects

All the cases of family PAK-CMT1-DG KHAN were born with full-term pregnancy from healthy parents, and there was no family history of the disease. All the affected subjects had early and severe disease onset. The enrolled cases were unable to walk and had clumsiness at young age progressing to wheelchair requirement. Subjects had bowed arms and legs with affected backbones (scoliosis). All the cases also presented pes cavus, loss of dexterity, and affected hand grip. Intelligence and facial appearances were normal (Fig. 1 and Table 1).

All the cases of family PAK-CMT2-LAYYAH were also born following the completion of a normal, full-term, and uneventful pregnancy. Their parents were normal and healthy with no family history of disease. CMT-affected subjects had an early onset of disease, and they presented bowed arms and legs with pes cavus. Movement was difficult and painful, and hand grip was severely affected with an overall muscular weakness. No scoliosis was observed in these subjects. Intelligence and facial appearances were normal (Fig. 1 and Table 1).

Electrophysiological findings

Nerve conduction study (NCS) revealed that SNCVs and MNCVs for both families were <38 m/s. Motor nerve conduction studies revealed prolonged latency, low amplitude, and slow conduction rates in median, ulnar, tibial, and peroneal nerves. While nerve conduction velocities were within the normal ranges for bilateral musculocutaneous motor nerves. Sensory nerve conduction studies also revealed prolonged latency, low amplitude, and slow conduction rates in bilateral median, ulnar, and sural sensory nerves. Individual variations among the patients are summarized in Table 2.

EMG of the FDI, ABP, TA, VL, brachioradialis, and biceps muscles of the four patients revealed similar findings. Analyzed muscles showed frank denervation, neuropathic motor unit potential, and reduced interference pattern with very poor to moderate effort.

GDAP1 *gene mutation*

WES generated ~65,536 variants in the PAK-CMT1-DG KHAN family. All suspected variants were confirmed by Sanger sequencing. A single candidate gene, *GDAP1*, was identified with recessive mode of inheritance. A homozygous G to T change at nucleotide position 226 (c. 226 G>T) in exon 6 was detected in all the affected individuals of this family causing autosomal recessive Charcot–Marie–Tooth disease type 4A (CMT4A). This mutation generated a premature termination codon at AA 76. Normal siblings were heterozygous for this mutation (Fig. 2).

MFN2 *gene mutation*

WES followed by Sanger sequencing revealed a homozygous G to A change at nucleotide position 334 (c. 334 G>A) in exon 4 of *MFN2* gene in all the affected individuals of family PAK-CMT2-LAYYAH. This mutation resulted in valine to methionine AA change at position 112 (p. Val 112

Table 1. Genotype and Phenotype Correlation of the Two Families Enrolled in the Present Study from Punjab (Pakistan)

Family	*Gene/mutation*	*CMT type*	*Pedigree position*	*Gender/ phenotype*	*Genotype*	*Age at sample collection/disease onset (years)*	*Arms and legs/ pes cavus*	*Movement/hand grip*	*Scoliosis*
PAK-CMT1-DG KHAN	*GDAP1*/c. 226 G>T p. Glu 76X	CMT4A	IV 3	Female/normal	GT	35/—	Normal/no	Normal/normal	No
			IV 4	Male/normal	GT	36/—	Normal/no	Normal/normal	No
			IV 5	Female/normal	GT	34/—	Normal/no	Normal/normal	No
			IV 6	Male/normal	GT	37/—	Normal/no	Normal/normal	No
			V 1	Male/normal	GT	12/—	Normal/no	Normal/normal	No
			V 2	Male/CMT	TT	07/By birth	Bowed/yes	Unable to walk/weak	No
			V 3	Female/CMT	TT	14/<01	Bowed/yes	Unable to walk/weak	Yes
			V 4	Female/CMT	TT	09/<01	Bowed/yes	Unable to walk/weak	Yes
			V 5	Male/CMT	TT	12/<01	Bowed/yes	Unable to walk/weak	Yes
			V 6	Male/CMT	TT	08/<01	Bowed/yes	Unable to walk/weak	Yes
PAK-CMT2-LAYYAH	*MFN2*/c. 334 G>A p. Val 112 Met	CMT2A	III 2	Male/normal	GA	45/—	Normal/no	Normal/normal	No
			III 3	Female/normal	GA	40/—	Normal/no	Normal/normal	No
			III 5	Female/normal	GA	29/—	Normal/no	Normal/normal	No
			III 6	Male/normal	GA	43/—	Normal/no	Normal/normal	No
			III 7	Female/normal	GA	35/—	Normal/no	Normal/normal	No
			IV 4	Male/CMT	AA	12/<01	Bowed/yes	Slow and painful/weak	No
			IV 6	Female/CMT	AA	10/<01	Bowed/yes	Slow and painful/weak	No
			IV 9	Male/CMT	AA	15/<01	Bowed/yes	Slow and painful/weak	No
			IV 11	Female/CMT	AA	08/<01	Bowed/yes	Slow and painful/weak	No

AA, amino acids; CMT, Charcot–Marie–Tooth disease; CMT2A, Charcot–Marie–Tooth disease type 2A; CMT4A, Charcot–Marie–Tooth disease type 4A.

Table 2. Clinical Features of the Four Pakistani Charcot–Marie–Tooth Disorder Patients Enrolled in the Present Study

Parameter	*PAK-CMT1-DG KHAN: V-4 (Female)*	*PAK-CMT1-DG KHAN: V-5 (Male)*	*PAK-CMT2-LAYYAH: IV-4 (Male)*	*PAK-CMT2-LAYYAH: IV-6 (Female)*
Motor nerve conduction studies				
Median MNCV (m/s)	17.5	19.9	12.6	18.2
Latency	Prolonged	Normal	Normal	Normal
Amplitude	Low	Low	Low	Low
F-wave	Absent	Absent	Absent	Absent
Ulnar MNCV (m/s)	17.9	15.7	16.9	19.9
Latency	Prolonged	Normal	Prolonged	Prolonged
Amplitude	Low	Low	Low	Low
F-wave	Absent	Absent	Absent	Absent
Peroneal MNCV (m/s)	12.9	12.6	12.3	11.5
Latency	Prolonged	Prolonged	Normal	Prolonged
Amplitude	Low	Low	Low	Low
F-wave	Absent	Absent	Absent	Absent
Musculocutaneous MNCV (m/s)	29.1	33.7	66.7	61.1
Latency	Prolonged	Normal	Normal	Prolonged
Amplitude	Low	Normal	Normal	Normal
Tibial MNCV (m/s)	10.3	11.2	11.9	11.0
Latency	Prolonged	Prolonged	Normal	Prolonged
Amplitude	Low	Low	Low	Low
F-wave	Absent	Absent	Absent	Absent
Sensory nerve conduction studies				
Median SNCV (m/s)	26.5	16.0	24.7	24.7
Latency	Prolonged	Prolonged	Prolonged	Prolonged
Amplitude	Low	Low	Low	Low
Ulnar SNCV (m/s)	23.3	17.3	20.3	20.3
Latency	Prolonged	Prolonged	Prolonged	Prolonged
Amplitude	Normal	Low	Low	Low
Sural SNCV (m/s)	32.6	23.6	36.6	36.6
Latency	Normal	Prolonged	Normal	Prolonged
Amplitude	Low	Low	Normal	Low

MNCV, motor nerve conduction velocity; SNCV, sensory nerve conduction velocity.

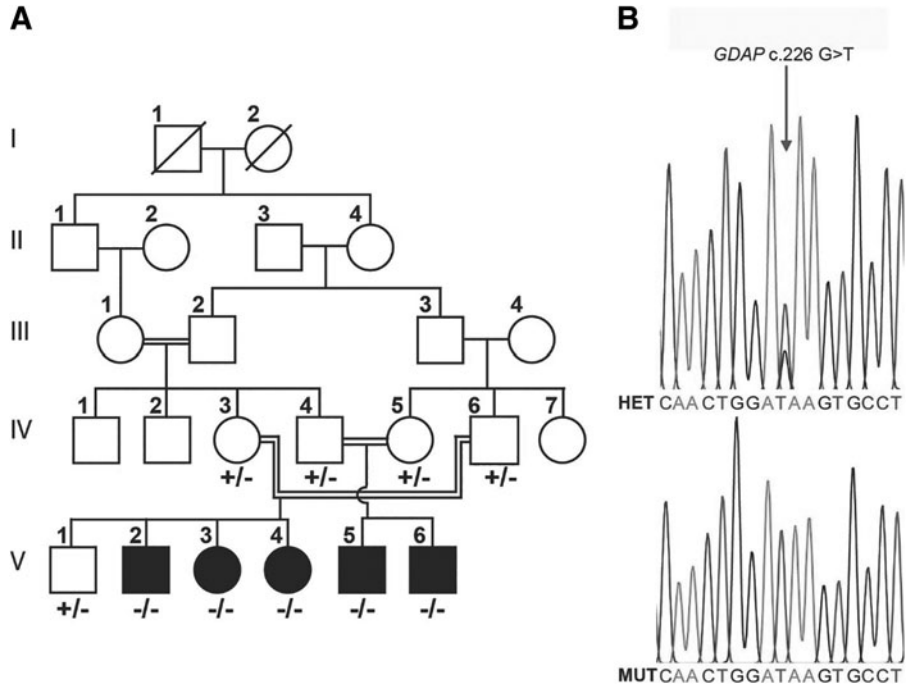

FIG. 2. **(A)** Pedigree of family PAK-CMT1-DG KHAN presenting the genotype at nucleotide position 226 (G>T) in exon 6 of *GDAP1* gene. Following the recessive mode of inheritance, all normal subjects (IV-3, IV-4, IV-5, IV-6, and V-1) carried heterozygous alleles (G/T), while the affected individuals (V-2, V-3, V-4, V-5, and V-6) carried homozygous mutant alleles (T/T). Mutation in family members was confirmed by Sanger sequencing. **(B)** Chromatogram for *GDAP1* selected region showing c.226 G > T transition. GDAP1, ganglioside-induced differentiation-associated protein 1.

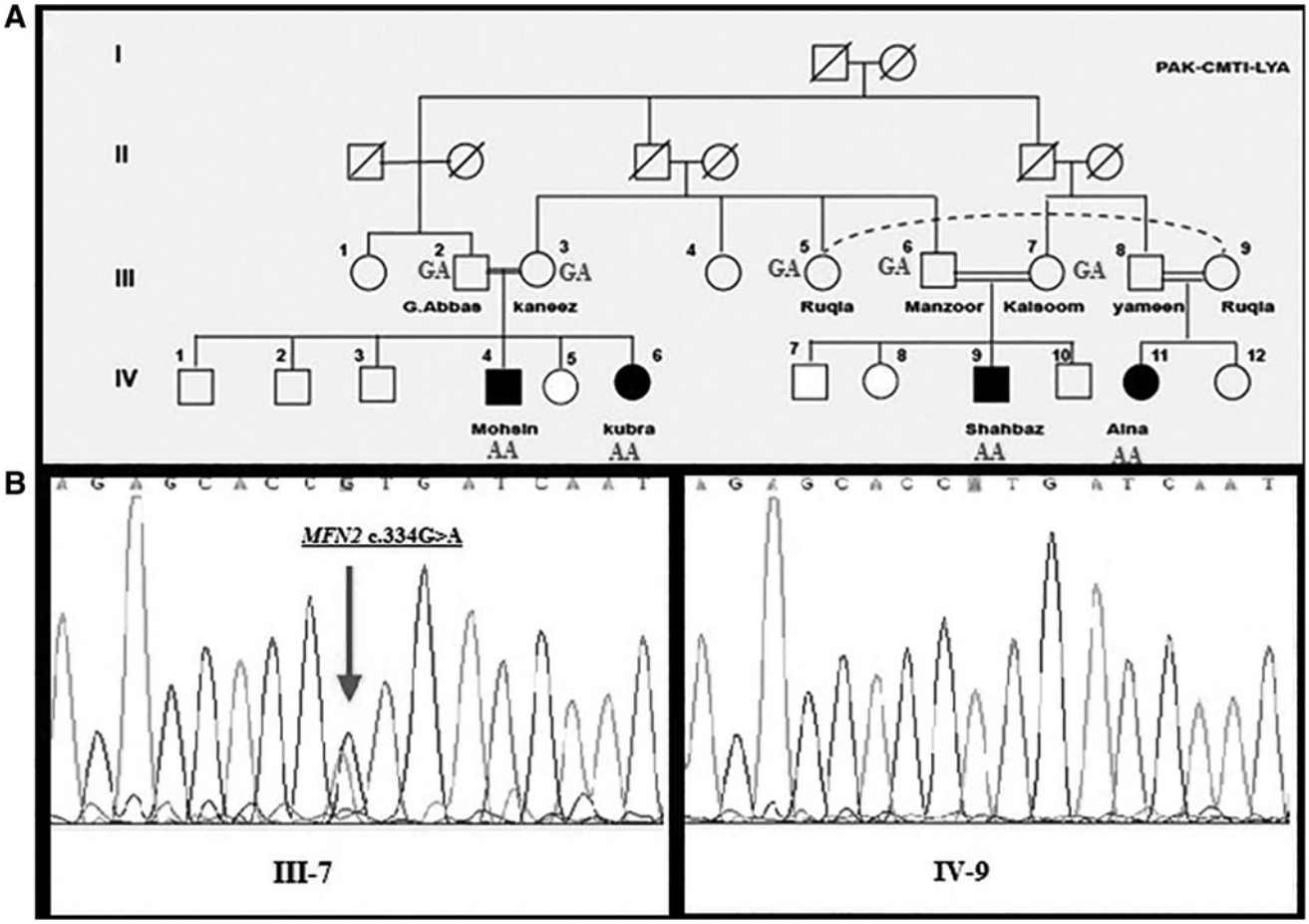

FIG. 3. **(A)** Pedigree of family PAK-CMT2-LAYYAH presenting the genotype at nucleotide position 334 (G>A) in exon 4 of *MNF2* gene. Following the recessive mode of inheritance, all normal subjects (III-2, III-3, III-5, III-6, and III-7) carried heterozygous alleles (G/A), while the affected individuals (IV-4, IV-6, IV-9, and IV-11) carried homozygous mutant alleles (A/A). Mutation in family members was confirmed by Sanger sequencing. **(B)** Chromatogram for *GDAP1* selected region showing c. 334 G > A transition. MNF2, Mitofusin-2.

Met) resulting in the development of autosomal recessive Charcot–Marie–Tooth disease type 2A (CMT2A). Normal siblings were heterozygous for this mutation (Fig. 3).

Multiple sequence alignment analysis

Clustal Omega analysis revealed that glutamine in GDAP1 and valine in MNF2 along with other AAs in the targeted domains of these protein domains are highly conserved among the vertebrates (Supplementary Fig. S1), and any mutation in this region may lead to profound effects on the phenotype of the subjects.

In silico *mutation stability analysis*

ENCoM model analysis revealed that both mutated models –0.188 (ΔΔG) (GDAP1_E76T) and –0.207 (ΔΔG) (MNF2_V112M) showed negative values indicating the destabilizing behavior of the affected proteins. Moreover, both mCSM and SDM predicted results with negative values –0.090, –0.333 and –0.650, –0.800 for GDAP1_E76T and MNF2_V112M, respectively, confirming the destabilizing behavior of protein models (Table 3). DUET analysis indicated stable GDAP1_E76T behavior with 0.076 (ΔΔG), whereas MNF2_V112M showed 0.228 (ΔΔG) with destabilizing conformational effect (Table 3).

Table 3. Effect of Detected Mutations in GDAP1 and MNF2 Genes on Target Protein Stability

Mutated proteins models	*ENCoM (ΔΔG)*	*DUET (ΔΔG)*	*mCSM (ΔΔG)*	*SDM (ΔΔG)*	*Overall effect*
GDAP1_E76T	–0.188	0.076 (Stabilizing)	–0.090	–0.650	Destabilizing
MNF2_V112M	–0.207	–0.228	–0.333	–0.800	Destabilizing

ΔΔG represents the change in binding affinity of protein caused by the mutation.
GDAP1, ganglioside-induced differentiation-associated protein 1; MNF2, Mitofusin-2.

GDAP1 protein structural assessment

The GDAP1 is composed of 280 AAs, and VADAR analysis revealed that GDAP1 contains 46% helixes, 7% beta sheets, 45% coils, and 10% turns. Similarly, as the truncated protein model reduced its sequence length, the following values were observed: 26% helix, 22% beta sheets, 50% coils, and 16% turns. The MolProbity analysis of GADP1 showed that the generated Ramachandran graph depicts 95.5% of all residues in favored regions and 98.9% of all residues in allowed regions. In truncated protein, 96.1% of all residues were in favored regions and 100.0% of all residues were in allowed regions (Fig. 4).

Superimposition of predicted GDAP1 protein models

Structural superposition was employed to compare the conformation proteins with their structural insights, such as α-helices, β-sheets, and loops. As the model proteins have bigger difference in their total length of AAs, and as the mutated protein was truncated, a little conserved conformational pattern was observed (Fig. 5A, B). In detailed matchmaker GDAP1-truncated protein result, the sequence alignment score was 270.2. Whereas the root-mean-square deviation between 49 pruned atom pairs was 0.416 Å. In comparative analysis, it was observed that most part of the remaining truncated protein structure was properly superimposed, whereas some loop region showed little deviation from the wild-type protein, which may lead to alter the GDAP1 function through the activation or deactivation of the downstream signaling pathways. The surface representation of both model structures is depicted in Figure 5C.

MNF2 protein structural assessment

The comparative analysis of MNF2 protein models showed little fluctuation at mutation site where valine was substituted by methionine AA (Fig. 6A, B).

Discussion

The GDAP1 belongs to the ganglioside-induced differentiation-associated protein family usually expressed in central tissues of the nervous system not only in neurons but also in Schwann cells (Niemann et al., 2005). This protein family is known to play a role in the signal transduction pathway during neuronal development, and mutations in this gene have previously been linked with CMT and other neuropathies (Cuesta et al., 20021). By using embryonic motor neuron cultures from *Gdap1*-knockout mouse, Civera-Tregon et al. (2021) recently reported that the loss of GDAP1 critically compromises the morphology and function of mitochondria and its relationship with the calcium homeostasis in the soma and axons of the studied neurons that lead to axonal degeneration during *GDAP1*-related CMT neuropathies.

CMT is divided into two basic types of neuropathy: demyelinating and axonal. CMT1 is the clinical diagnosis for demyelinating CMT, and CMT2 is the clinical diagnosis for axonal CMT (Kanwal et al., 2021). Each is determined by the NCS results. The NCS general rule-of-thumb for demyelinating CMT is nerve conduction velocities <38 m/s, while for axonal CMT, these values are >38 m/s (Fridman et al., 2015). In the present study, we found a novel mutation (c. 226 G>T) in *GDAP1* gene that resulted in generation of a truncated GDAP1 protein causing CMT in enrolled family PAK-CMT1-DG KHAN (Fig. 2). Electrophysiological analysis of the patients revealed that they were suffering from demyelinating type of CMT as the nerve conduction velocities were <38 m/s. The enrolled subjects had the early onset of severe, rapidly progressing sensorimotor neuropathy that initially affected the distal lower extremities and later the proximal muscles and upper extremities.

Clinical correlation with electrophysiological findings revealed that these subjects were suffering from CMT4A. Recently, Miressi et al. (2021) documented the importance of GADP1 functioning during normal motor neuron activity.

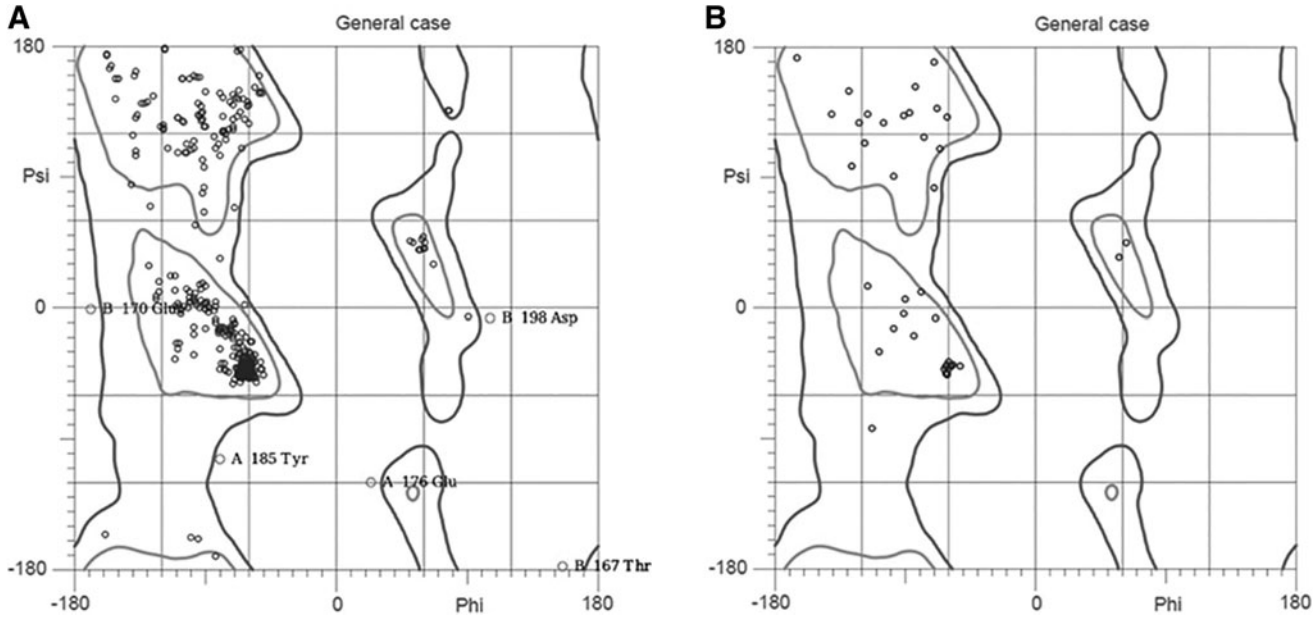

FIG. 4. Ramachandran graphs for predicted GDAP1 protein models. **(A)** Wild type and **(B)** truncated GDAP1 protein.

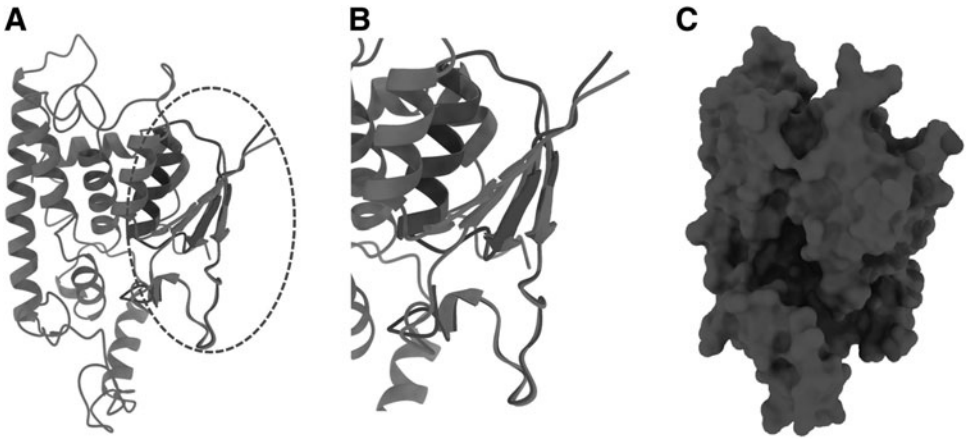

FIG. 5. **(A, B)** Predicted models of GADP1 (*grey*) and truncated proteins (*dark grey*) with superimposition. Loop region showed little deviation, whereas α-helices and β-sheets showed good alignment in superimposition. **(C)** Predicted models of GADP1 and truncated proteins in surface format.

They used the human induced pluripotent stem cell-derived motor neurons that were obtained from a CMT2H patient who was homozygous for c.581C>G (p.Ser194*) mutation in *GDAP1* gene and reported drastically reduced mRNA expression in motor neurons and a decreased cellular viability due to lipid dysfunction and development of oxidative stress. Mutations in *GDAP1* gene have been reported to be associated with both autosomal recessive demyelinating CMT4A and axonal CMT with vocal cord paralysis (Nelis et al., 2002). Kabzińska et al. (2007) presented a case report of a 32-year-old Polish male who was born in a consanguineous family and developed gait problem that restricted his movement by the age of 4 years followed by progressive lower limb atrophy.

Genetic analysis revealed a homozygous c.458C>T substitution in the *GDAP1* gene of the subject resulting in the development of Charcot–Marie–Tooth disease type 4C4 (CMT4C4). In an earlier study, Kabzińska et al. (2006) reported Met116Thr in the *GDAP1* gene that led to the development of CMT4C4 in two Polish brothers who were born to non-consanguineous parents. The subjects had difficulty in walking during very early part of their life, and later on, they were unable to stand on their heels and had foot drops. Kabzińska et al. (2010) reported L239F mutation in the *GDAP1* gene in one Bulgarian and five Polish families causing CMT4C with a milder clinical entity with a long-preserved period of ambulance (till the end of the second decade of life).

Recently, Kim et al. (2021) reported *GDAP1* mutations in 10 Korean patients who belonged to 8 different families. They reported both autosomal dominant (in five families) and autosomal recessive (in three families) mode of inheritance in Korean population causing CMT type 2K and CMT type A, respectively. Lehtilahti et al. (2021) also reported that p.His123Arg in the *GDAP1* gene was the most common disease-causing mutation in patients with polyneuropathy in Finland. The subjects suffered from proximal muscle weakness of the lower extremities, and pes cavus was also common.

MFN2 gene encodes a protein that is part of mitochondrial membrane and plays its role in maintenance and mitochondrial network operations. Recently, it has been reported that MFN2 protein plays a role in mitochondria–endoplasmic reticulum tethering and mitochondrial trafficking along axons (Zanfardino et al., 2023). Mutations in *MFN2* can result in peripheral nervous system disorders including Charcot–Marie–Tooth disease type 2A2 and hereditary motor and sensory neuropathy VI (Kanwal et al., 2021). In the present study, all the affected subjects of family PAK-CMT2-LAYYAH were found homozygous for a previously known missense mutation (c. 334 G>A) in *MFN2* displaying an autosomal recessive mode of inheritance with more severe and earlier onset of CMT2A (MIM 617087) (Fig. 3).

Previously, most of the mutations in *MFN2* were found to be associated with dominant CMT2A2A (MIM 609260) (Züchner et al., 2004) or CMT6A (MIM 601152) (Züchner et al., 2006), but recently, Kanwal et al. (2021) reported a 7-year-old Pakistani boy suffering from severe form of CMT2A2B that had an early onset, and the subject harbored the same homozygous [c. 334G>A (p.Val112Met)] in *MFN2* with autosomal recessive mode of inheritance as reported in the present study. This mutation has already been reported with a very low frequency (1.6E-5) in the gnomAD and has been registered in the ClinVar database as likely to be pathogenic. Nicholson et al. (2008) also reported three single affected individuals with homozygous or compound heterozygous mutations in *MFN2* gene and having minimal clinical findings of neuropathy and minor electrophysiological evidence of neuropathy. All mutations described by Nicholson et al. (2008) were conserved and led to significant AA changes that resulted in a change in charge or hydrophobicity of the protein.

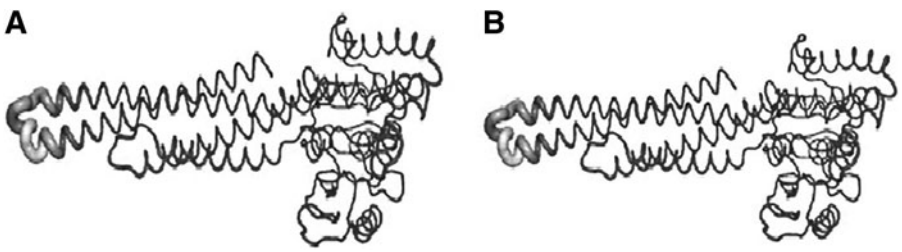

FIG. 6. Wild **(A)** and mutant model **(B)** of MNF2. The magnitude of the fluctuation is represented by thin to thick tube in *dark grey*, while *white* for moderate and *grey* represents the high magnitude of the fluctuation.

Larrea et al. (2019) used the fibroblasts from patients suffering from CMT2A due to different mutations in *MFN2*, and they reported disturbed endoplasmic reticulum and mitochondrial connectivity and altered mitochondria-associated endoplasmic reticulum membranes (MAM) and suggested that the severity of CMT2A can be correlated with the level of observed MAM alterations. However, respiratory chain function in the studied cells remained unimpaired. Amiott et al. (2008) also reported that mitochondrial membrane fusion and division are balanced processes that are necessary to maintain tubular mitochondrial morphology, respiratory function, and uniform distribution of the organelle throughout the cell, and these features are attributed to the normal MFN2 protein functioning, and *MFN2* gene mutations disturb this normal cell functioning leading to CMT2A.

Proteins are highly dynamic molecules, whose function is intrinsically linked to their molecular structures. Predicting the structure and thermodynamics of protein–protein interactions is key to a proper understanding and modulation of their function. The binding affinity change caused by mutations (i.e., $\Delta\Delta G$) is defined as the difference of binding affinity between the mutant and wild-type protein complexes (Geng et al., 2019). In the present investigation, a number of integrated computational approaches including ENCoM, mCSM, SDM, and DUET were used to report the mutational effect in GDAP1 and MNF2 proteins by applying consensus prediction using the Support Vector Machine method (Hassan et al., 2017; Pires et al., 2014a and b).

These approaches generate $\Delta\Delta G$ that can have positive and negative values, where positive prediction represents the stabilized structural morphology and negative values depict destabilized protein behavior. Analysis of our results indicated that both the mutations that are detected in the present investigation are capable of destabilizing the GDAP1 and MNF2 proteins that may change conformation of protein and their associated signaling pathways (Table 3).

The 3D conformations of a protein influence its function and affect the ligand selection to which this protein can interact. During this protein–ligand complex formation, the total free energy changes include enthalphic and entropic components, which together report on the binding affinity and conformational states of the complex (Chen et al., 2022). In the present investigation, we found that a homozygous change at nucleotide position 226 (c. 226 G>T) in *GDAP1* gene resulted in premature termination codon that produced a truncated protein causing CMT in family PAK-CMT1-DG KHAN (Figs. 2 and 5). It has already been documented that protein truncation is irreversible modification, which has been postulated to have a great impact on generating diversity in the human proteome and to increase the functional repertoire of proteins by precise alteration in the biological properties of proteins (Fortelny et al., 2015).

Genetic analysis of family PAK-CMT2-LAYYAH revealed a missense mutation 334 (c. 334 G>A) in *MFN2* that resulted in valine to methionine AA (Fig. 6A, B). Such residual disturbance in the protein structure may cause major change in the conformational behavior of protein structure especially in substructure regions, such as α-helices, β-sheets, and loops (Huang et al., 2019). Therefore, we can predict that residual disturbance in the analyzed protein structures may cause major change in the conformational behavior of protein structure especially in substructure regions, such as α-helices, β-sheets, and loops. These changes may be the trigging factors in the activation or deactivation of signaling pathways resulting in CMT in enrolled subjects.

In conclusion, we report that a novel nonsense mutation (c. 226 G>T) in *GADP1* gene and a previously known missense mutation in *MFN2* gene (c. 334 G>A) cause autosomal recessive CMT4A in the PAK-CMT1-DG KHAN family and autosomal recessive CMT2A in the PAK-CMT2-LAYYAH family, respectively. We believe that our findings will contribute to understanding the genetic basis of peripheral neuropathy and will help in improving the molecular diagnostics and treatment options for CMT.

Acknowledgments

We thank Dr. Hao Yu at the Second Affiliated Hospital, Zhejiang University School of Medicine, Hangzhou, China, Dr. He Jin at the First Affiliated Hospital, Fujian Medical University, China, and Dr. Jun Wang at the Life Sciences Institute, Zhejiang University, China, for their technical support in this study.

Authors' Contributions

F.I. and C.-C.Che. designed, supervised, and prepared the article. M.A., M.F.H., and M. Hu located the families, collected the blood sample, epidemiological, and clinical data. A.K. and N.N. performed laboratory experiments. M.G. and M.H. performed the nerve conduction study and electromyography. A.Kl. and M. Ha performed the *in silico* analysis and protein structure analysis. Z.S. and C.C.Chi. performed the sequence alignment and drew the pedigrees. All authors have revised and approved the article for submission.

Data Availability

All the raw WES data associated with this study are available in the Sequence Read Archive (SRA) of the National Center for Biotechnology Information under the accession number PRJNA962009 (https://www.ncbi.nlm.nih.gov/sra/PRJNA962009).

Disclosure Statement

No competing financial interests exist.

Funding Information

This research was funded by Ditmanson Medical Foundation Chia-Yi Christian Hospital, through grant number R112-22 awarded to Chien-Chun Chiou and Chien-Chin Chen.

Supplementary Material

Supplementary Data S1 CMTI patient data
Supplementary Figure S1

References

Amiott EA, Lott P, Soto J, et al. Mitochondrial fusion and function in Charcot-Marie-Tooth type 2A patient fibroblasts with mitofusin 2 mutations. Exp Neurol 2008;211(1):115–127.

Chen X, Leyendecker S, van den Bedem H. Kinematic vibrational entropy assessment and analysis of SARS CoV-2 main protease. J Chem Info Model 2022;62(11):2869–2879.

Civera-Tregón A, Domínguez L, Martínez-Valero P, et al. Mitochondria and calcium defects correlate with axonal dysfunction in GDAP1-related Charcot-Marie-Tooth mouse model. Neurobiol Dis 2021;152:105300; doi: 10.1016/j.nbd.2021.105300

Cuesta A, Pedrola L, Sevilla T, et al. The gene encoding ganglioside-induced differentiation-associated protein 1 is mutated in axonal Charcot-Marie-Tooth type 4A disease. Nat Genet 2002;30(1):22–25.

Frappier V, Chartier M, Najmanovich RJ. ENCoM server: Exploring protein conformational space and the effect of mutations on protein function and stability. Nucleic Acid Res 2015;43(W1):W395–W400.

Fridman V, Bundy B, Reilly MM, et al. CMT subtypes and disease burden in patients enrolled in the Inherited Neuropathies Consortium natural history study: A cross-sectional analysis. J Neurol Neurosurg Psychiatry 2015;86:873–878.

Fortelny N, Pavlidis P, Overall CM. The path of no return-truncated protein N-termini and current ignorance of their genesis. Proteomics 2015;15(14):2547–2552.

Geng, C, Xue, LC, Roel-Touris J et al. Finding the $\Delta\Delta G$ spot: Are predictors of binding affinity changes upon mutations in protein–protein interactions ready for it? WIREs Comput Mol Sci 2019;9:e1410; doi: 10.1002/wcms.1410

Hassan M, Abbas Q, Raza H, et al. Computational analysis of histidine mutations on the structural stability of human tyrosinases leading to albinism insurgence. Mol Biosyst 2017;13(8):1534–1544.

Higuchi Y, Takashima H. Clinical genetics of Charcot–Marie–Tooth disease. J Hum Genet 2023;68:199–214.

Houlden H, Laura M, Wavrant-De Vrièze F, et al. Mutations in the HSP27 (HSPB1) gene cause dominant, recessive, and sporadic distal HMN/CMT type 2. Neurology 2008;71:1660–1668.

Huang Q, Rodgers JM, Hemley RJ, et al. Effects of pressure and temperature on the atomic fluctuations of dihydrofolate reductase from a psychropiezophile and a mesophile. Int J Mol Sci 2019;20(6):1452.

Kabzińska D, Kochański A, Drac H, et al. A novel Met116Thr mutation in the GDAP1 gene in a Polish family with the axonal recessive Charcot–Marie–Tooth type 4 disease. J Neurol Sci 2006;241(1–2):7–11.

Kabzińska D, Saifi GM, Drac H, et al. Charcot-Marie-Tooth disease type 4C4 caused by a novel Pro153Leu substitution in the GDAP1 gene. Acta Myol 2007;26(2):108–111.

Kabzińska D, Strugalska-Cynowska H, Kostera-Pruszczyk A, et al. L239F founder mutation in GDAP1 is associated with a mild Charcot-Marie-Tooth type 4C4 (CMT4C4) phenotype. Neurogenetics 2010;11(3):357–366.

Kanwal S, Choi YJ, Lim SO, et al. Novel homozygous mutations in Pakistani families with Charcot-Marie-Tooth disease. BMC Med Genomics 2021;14(1):174.

Kim HS, Kim HJ, Nam SH, et al. Clinical and neuroimaging features in Charcot-Marie-Tooth patients with *GDAP1* mutations. J Clin Neurol 2021;17(1):52–62.

Larrea D, Pera M, Gonnelli A, et al. MFN2 mutations in Charcot-Marie-Tooth disease alter mitochondria-associated ER membrane function but do not impair bioenergetics. Hum Mol Genet 2019;28(11):1782–1800.

Lehtilahti M, Kallio M, Majamaa K, et al. Phenotype of patients with Charcot-Marie-Tooth with the p.His123Arg Mutation in *GDAP1* in Northern Finland. Neurol Genet 2021;7(6):e629 doi: 10.1212/NXG.0000000000000629

Miressi F, Benslimane N, Favreau F, et al. GDAP1 involvement in mitochondrial function and oxidative stress, investigated in a Charcot-Marie-Tooth model of hiPSCs-Derived Motor Neurons. Biomedicines 2021;9:945.

Mustafa S, Akhtar Z, Asif M, et al. Novel missense variants in FGFR1 and FGFR3 causes short stature in enrolled families from Pakistan. Meta Gene 2020;26:100778; doi: 10.1016/j.mgene.2020.100778

Nelis E, Erdem S, Van Den Bergh PY, et al. Mutations in GDAP1: Autosomal recessive CMT with demyelination and axonopathy. Neurology 2002;59(12):1865–1872.

Nicholson GA, Magdelaine C, Zhu D, et al. Severe early-onset axonal neuropathy with homozygous and compound heterozygous MFN2 mutations. Neurology 2008;70(19):1678–1681.

Niemann A, Ruegg M, La Padula V, et al. Ganglioside-induced differentiation associated protein 1 is a regulator of the mitochondrial network: New implications for Charcot-Marie-Tooth disease. J Cell Biol 2005;170(7):1067–1078.

Pedurupillay CR, Amundsen SS, Barøy T, et al. Clinical and molecular characteristics in three families with biallelic mutations in IGHMBP2. Neuromuscul Disord 2016;26(9):570–575.

Pettersen EF, Goddard TD, Huang CC, et al. UCSF Chimera—A visualization system for exploratory research and analysis. J Comput Chem 2004;25(13):1605–1612.

Pires DE, Ascher DB, Blundell TL. DUET: A server for predicting effects of mutations on protein stability using an integrated computational approach. Nucleic Acid Res 2014a;42(Web Server issue):W314–W319.

Pires DE, Ascher DB, Blundell TL. mCSM: Predicting the effects of mutations in proteins using graph-based signatures. Bioinformatics 2014b;30(3):335–342.

Pisciotta C, Saveri P, Pareyson D. Challenges in treating Charcot-Marie-Tooth disease and related neuropathies: Current management and future perspectives. Brain Sci 2021;11(11):1447.

Rodrigues CH, Pires DE, Ascher DB. DynaMut: Predicting the impact of mutations on protein conformation, flexibility and stability. Nucleic Acid Res 2018;46(W1):W350–W355.

Studer G, Tauriello G, Bienert S, et al. ProMod3—A versatile homology modelling toolbox. PLoS Comp Biol 2021;17(1):e1008667.

Worth CL, Preissner R, Blundell TL. SDM—A server for predicting effects of mutations on protein stability and malfunction. Nucleic Acid Res 2011;39(Web Server issue):W215–W222; doi: 10.1093/nar/gkr363

Wright GC, Brown R, Grayton H, et al. Clinical and radiological characterization of novel FIG4-related combined system disease with neuropathy. Clin Genet 2020;98:147–154.

Zambon AA, Natali Sora MG, Cantarella G, et al. Vocal cord paralysis in Charcot–Marie–Tooth type 4b1 disease associated with a novel mutation in the myotubularin-related protein 2 gene: A case report and review of the literature. Neuromuscul Disord 2017;27: 487–491.

Zanfardino P, Longo G, Amati A, et al. Mitofusin 2 mutation drives cell proliferation in Charcot-Marie-Tooth 2A fibroblasts. Hum Mol Genet 2023;32(2):333–350.

Zhou Q, Yang D, Ombrello AK, et al. Early-onset stroke and vasculopathy associated with mutations in ADA2. N Engl J Med 2014;370(10):911–920.

Züchner S, De Jonghe P, Jordanova A, et al. Axonal neuropathy with optic atrophy is caused by mutations in mitofusin 2. Ann Neurol 2006;59:276–281.

Züchner S, Mersiyanova IV, Muglia M, et al. Mutations in the mitochondrial GTPase mitofusin 2 cause Charcot–Marie–Tooth neuropathy type 2A. Nat Genet 2004;36: 449–451.

Address correspondence to:
Furhan Iqbal, PhD
Institute of Zoology
Bahauddin Zakariya University
Bosan Road
Multan 60800
Pakistan

E-mail: furhan.iqbal@bzu.edu.pk

Chien-Chin Chen, MD, FIAC
Department of Pathology
Ditmanson Medical Foundation Chia-Yi
Christian Hospital
No. 539, Zhongxiao Road
East District
Chiayi 600
Taiwan

E-mail: hlmarkc@gmail.com

Received for publication May 3, 2023; received in revised form July 9, 2023; accepted August 23, 2023.